**Proceedings of the ASME 2011 9th International Conference on Nanochannels, Microchannels, and Minichannels**
**ICNMM2011**
**June 19-22, 2010, Edmonton, Alberta, Canada**

# ICNMM2011-58022

# DSMC SIMULATION OF PRESSURE DRIVEN BINARY RAREFIED GAS FLOWS THROUGH SHORT MICROTUBES

**Lajos Szalmas [1,2], Dimitris Valougeorgis [2] and Stephane Colin [1]**
[1] Universite de Toulouse, Institut National des Sciences Appliquees, 135 Avenue de Rangueil, Toulouse, F-31077 France
[2] Department of Mechanical Engineering, University of Thessaly, Volos, 38334 , Greece
Email: szalmas@insa-toulouse.fr, stephane.colin@insa-toulouse.fr, diva@mie.uth.gr

## ABSTRACT

*Binary gas flows driven by pressure gradient through short microtubes are studied by using an upgraded version of the Direct Simulation Monte Carlo (DSMC) method. Two types of mixtures, $He/Xe$ and $Ne/Ar$, are examined. Several values of the channel length to radius ratio, the downstream to upstream pressure ratio and a wide range of the gas rarefaction are considered. Results are presented for the species and total flow rates and for the axial distributions of the macroscopic quantities. There is a pronounced difference of the flow behavior of the two mixtures due to the different molecular mass ratios. The flow rate of the $He/Xe$ mixture for very short channels and large pressure drops is increased with increasing gas rarefaction, while the flow rate of the $Ne/Ar$ mixture shows a different rarefaction dependence. The obtained results can be useful in optimal design of microfluidic or vacuum devices.*

## INTRODUCTION

Binary gaseous mixture flows through various short tubes have great importance in science and technology. Such flows can be found in vacuum technology, gas metrology, microfluidics among many others.

These flows may cover a wide range of the rarefaction interval from the viscous to the free molecular limit. In the viscous region, fluid dynamics or extended hydrodynamics may be used; however, for the whole range of the gas rarefaction a kinetic type description is necessary. Also, a relatively large set of flow parameters, such as the mixture type, the concentration, the pressure drop, the rarefaction degree and the channel length to radius ratio, are involved to characterize the problem.

Previous works both experimental and computational have mainly focused on single component gas flows through short tubes. First, Hanks and Weissberg studied flows through short capillaries [1]. They developed a flow rate formula in the hydrodynamic region taking into account the slip at the walls. Sreekanth investigated flow through short circular tubes experimentally by providing the flow rates in the slip and transition regions [2]. In addition, a flow rate formula has been derived and compared to the results of the measurements yielding good agreement. Borisov et al. [3] and Porodnov et al. [4] carried out measurement for flow through orifices, which is the limiting case of short tubes. Those works focused on small pressure drop, but a wide range of the gas rarefaction was covered. Fujimoto and Usami measured the mass flow rate through various short tubes in a wide range of the gas rarefaction by using an unsteady flow rate measurement technique [5]. Then, Usami and Okuyama investigated supersonic jets through orifices by applying the DSMC method [6]. Shinagawa et al. studied rarefied gas flow through short tubes experimentally and computationally by using the DSMC method [7]. Also, Lilly et al. have studied the effect of the channel length on the flow through thin orifices [8]. Recently, the DSMC method has been used to compute the flow for a wide range of the rarefaction through orifices [9], short tubes into vacuum [10] and short tubes at any pressure drop [11]. Since previous works have focused on single component gases, it is useful to study binary gas flow trough short tubes.

Flows of single gases and binary gaseous mixtures through

very long channels have been extensively studied in the past. In this case, the flow speed is usually small compared to the sound speed; as a result, linearized kinetic description can be used [12–15]. In addition, the McCormack collision term [16] among other models [17] has been used to describe the gaseous mixture flow. The corresponding kinetic equations have been solved for various flow configurations [18–22]. Although flows of binary gas mixtures through long channels have thoroughly been studied previously, corresponding work on short channels is missing. For short channels, the linearized description is not applicable.

In this paper, an upgraded DSMC method is developed to study binary rarefied gas flows through short tubes with various length to radius ratios. In order to study the effect of the molecular mass ratio, which turns out to be very important, two mixtures, namely $He/Xe$ and $Ne/Ar$, with quite different molecular mass ratios are analyzed. The simulations cover several channel length to radius ratios, various pressure ratios and a wide range of the rarefaction interval. The flow rates of each species and of the mixture are tabulated for the various flow parameters. In addition, typical profiles of the macroscopic quantities of density, axial velocity and temperatures together with the normalized rarefaction parameter and the Mach number are presented.

## 1 Definition of the problem

Binary gas flow through a short tube between an upstream and a downstream reservoir is considered. The flow is driven by the pressure difference between the containers. The radius and the length of the tube are denoted by $R$ and $L$, respectively. The flow configuration is axial-symmetric with respect to the channel axis. The axis of the tube lies in the $x'$ coordinate direction, while the radial coordinate is denoted by $r'$.

The mixture consists of two components $\alpha = [1,2]$ having molecular masses $m_\alpha$ and molecular diameters $d_\alpha$. In this work, it is always assumed that the first species is the lighter component. The number densities of the components are denoted by $n_\alpha$. The total number density of the mixture is introduced by $n = n_1 + n_2$. The concentration of the first component is given by

$$C = \frac{n_1}{n}. \tag{1}$$

It is mentioned that the concentration is a local quantity, and it varies in the flow domain. The concentration in the upstream reservoir $C_A$ is used as a reference value, while $C_B$ is the concentration in the downstream reservoir and it is taken equal to the upstream value, i.e., $C_A = C_B$. The gas pressure is denoted by $P$. The pressures in the upstream and downstream reservoirs are $P_A$ and $P_B$, respectively. The temperature is denoted by $T$ and its values in the two reservoirs $T_A$ and $T_B$ are taken to be equal to a reference temperature $T_0$ ($T_A = T_B = T_0$).

The flow is characterized by the rarefaction parameter

$$\delta = \frac{PR}{\mu(C)\nu(C)}. \tag{2}$$

Here, $\mu(C)$ is the mixture viscosity and $\nu(C)$ is the characteristic molecular velocity defined as

$$\nu(C) = \sqrt{\frac{2kT}{m(C)}}, \tag{3}$$

where $k$ is the Boltzmann constant and $m(C) = Cm_1 + (1-C)m_2$ is the average mass of the mixture. The rarefaction parameter is also a local quantity in the flow domain. Its value in the upstream reservoir

$$\delta_A = \frac{P_A R}{\mu_0(C_A)\nu_0(C_A)} \tag{4}$$

is used as a reference to characterize the flow problem. Here, the reference characteristic velocity $\nu_0(C_A) = \sqrt{2kT_0/m(C_A)}$ and the viscosity $\mu_0(C_A)$ are introduced on the basis of the reference upstream concentration $C_A$ and temperature $T_0$.

One of the interests of the present problem is in the component flow rates through the tube $J'_\alpha$ defined as

$$J'_\alpha = \int_{A'} n_\alpha u'_{\alpha x} dA', \tag{5}$$

where $u'_{\alpha x}$ is the axial component of the macroscopic gas velocity of species $\alpha$ and the integration refers to the inlet cross section $A'$. For convenience, the dimensionless flow rates are introduced by

$$J_\alpha = \frac{J'_\alpha}{n_A A' \nu_0(C_A)}, \tag{6}$$

where $n_A$ is the total number density in the upstream reservoir. The total flow rate of the mixture is $J = J_1 + J_2$.

## 2 The numerical method

In the present work, the DSMC method is employed to calculate the binary gas flow. The method seems the best choice for our purposes since the macroscopic gas velocities are not small for flows through short channels. As a consequence, the nonlinear Boltzmann equation is needed to be solved. This task can be fulfilled by the DSMC method in a computationally efficient

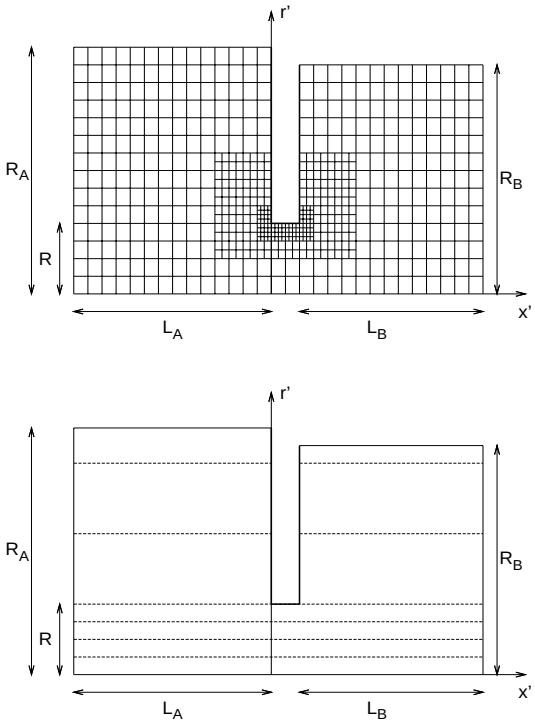


**FIGURE 1**. COMPUTATIONAL DOMAIN WITH THE THREE-LEVEL GRID (TOP) AND THE RADIAL AND AXIAL WEIGHTING ZONES (BOTTOM).

manner. The DSMC is a particle based method, actually a gas model [23]. However, in the limiting case, it solves the Boltzmann equation [24]. It has been successfully used for rarefied gas calculation over the last years. Various research groups have developed DSMC algorithms for general purposes [25, 26].

### 2.1 Computational algorithm

The binary flow through a short tube of radius $R$ and length $L$ between two cylindrical reservoirs having radii $R_A$, $R_B$ and heights $L_A$, $L_B$, is considered. The geometry is divided into a collection of cells. For a better resolution, the three-level grid presented in Fig. 1 is used in the present work. Near the tube, where the spatial variation of the bulk quantities is expected to be larger, the resolution of the grid is finer. The second-level grid is applied to the region $-R \le x' \le 0$ with $0.5R \le r' \le 2R$, $0 \le x' \le L$ with $0.5R \le r' \le R$ and $L \le x' \le R+L$ with $0.5R \le r' \le 2R$ for the upstream cylinder, the tube and the downstream cylinder. The third-level mesh refers to the region $-0.25R \le x' \le 0$ with $0.75R \le r' \le 1.25R$, $0 \le x' \le L$ with $0.75R \le r' \le R$ and $L \le x' \le 0.25R+L$ with $0.75R \le r' \le 1.25R$ for the same zones as in the case of the second-level mesh. In order to efficiently simulate the problem, radial and axial weighting zones are also applied (Fig. 1). The delimiters for the radial and axial zones are $r' = [0.25R, 0.5R, 0.75R, R, 2R, 3R]$ and $x' = 0$, respectively.

At the beginning of the simulation, model particles are uniformly distributed in the upstream reservoir, the tube and the downstream reservoir. In the upstream container and the tube, the initial number density is $n_0 = n_A/F$, where $F$ is the number of model particles represented by one particle. The number density in the downstream reservoir is $n_0(P_B/P_A) = (n_A/F)(P_B/P_A)$ in accordance with the pressure ratio.

The motion of the particles is divided into a free-streaming and a collision stage. In the free-streaming stage, the particles move along rectilinear trajectories in accordance with their velocity. The time step of the scheme is denoted by $\Delta t$. Upon colliding with the tube wall or the internal walls of the cylinders, the particles undergo purely diffuse reflection with wall temperature $T_0$. In each time step, particles are leaving and entering at the external boundaries of the computational domain. The number of entering particles through the unit surface during time step $\Delta t$ for components $\alpha = [1,2]$ in the reservoirs $i = [A,B]$ are

$$N^{(i)}_{Ent,1} = n_A \frac{P_i}{P_A} C_A \sqrt{\frac{m(C_A)}{m_1}} \frac{v_0(C_A)}{2\sqrt{\pi}} \Delta t, \tag{7}$$

$$N^{(i)}_{Ent,2} = n_A \frac{P_i}{P_A} (1-C_A) \sqrt{\frac{m(C_A)}{m_2}} \frac{v_0(C_A)}{2\sqrt{\pi}} \Delta t. \tag{8}$$

In the collision stage, the intermolecular collisions between the particles are simulated in a probabilistic manner in the cells, while the macroscopic quantities of the gas are calculated in the sampling procedure. Both issues are addressed in the following subsections.

### 2.2 Collision treatment

The collision treatment is based on the No Time Counter scheme. Also, the hard-sphere molecular system is used for describing the binary gas mixture. The selection procedure is group dependent for the components. The preselected number of pairs for collision in the time step $\Delta t$ from components $\alpha$ and $\beta$ is given by

$$N_{\alpha\beta} = \frac{1}{2V_C} N_\alpha \overline{N}_\beta F (\sigma_{T,\alpha\beta})_{max} (v_{R,\alpha\beta})_{max} \Delta t, \tag{9}$$

where $V_C$ is the volume of the cell, $N_\alpha$ is the number of particles from component $\alpha$, $\overline{N}_\beta$ is its average value in the previous time steps for component $\beta$, $\sigma_{T,\alpha\beta}$ is the total collision cross section and $v_{R,\alpha\beta}$ is the relative velocity. The total collision cross section for hard spheres is given by $\sigma_{T,\alpha\beta} = \pi d^2_{\alpha\beta}$ with $d_{\alpha\beta} = (d_\alpha +$

$d_\beta)/2$. The acceptance-rejection method is used to obtain the final distribution for the number of collisions. The preselected pair is accepted (or not) for collision based on the probability $p = v_{R,\alpha\beta}/(v_{R,\alpha\beta})_{max}$.

In the simulations, the collision cross section is an input parameter, which needs to be connected to the spatial scale of the problem. This can be achieved by the inclusion of the rarefaction parameter into the formalism through the viscosity. Actually, the $\sigma_{T,11}$ collision cross section is determined. The remaining values of $\sigma_{T,\alpha\beta}$ are obtained by $\sigma_{T,12} = \sigma_{T,21} = \sigma_{T,11}(d_{12}/d_{11})^2$ and $\sigma_{T,22} = \sigma_{T,11}(d_{22}/d_{11})^2$. The component $\sigma_{T,11}$ can be obtained by

$$\sigma_{T,11} = 1.016034\frac{5}{16}\frac{\sqrt{\pi m_1 k T_0}}{\mu_0(1)}. \tag{10}$$

By using the definition of the rarefaction parameter, the characteristic velocity and the ideal gas law, Eq. (10) can be written as

$$\sigma_{T,11} = 1.016034\frac{5}{16}\sqrt{2\pi}\sqrt{\frac{m_1}{m(C_A)}}\frac{\delta_A}{n_A R}\frac{\mu_0(C_A)}{\mu_0(1)}. \tag{11}$$

This quantity depends on the ratio of the viscosities, which is dimensionless and can be obtained as outlined in the following. The viscosity is calculated from the Chapman Enskog theory. It can be written as $\mu_0(C) = \mu_1 + \mu_2$, where $\mu_1$ and $\mu_2$ are given in Ref. [18] as

$$\mu_\alpha = P_{0\alpha}\frac{\Psi_\beta + \nu^{(4)}_{\alpha\beta}}{\Psi_\alpha\Psi_\beta - \nu^{(4)}_{\alpha\beta}\nu^{(4)}_{\beta\alpha}}, \tag{12}$$

with $\Psi_\alpha = \nu^{(3)}_{\alpha\alpha} - \nu^{(4)}_{\alpha\alpha} + \nu^{(3)}_{\alpha\beta}$. In these expressions, $\alpha,\beta = 1,2$ and $\alpha \neq \beta$. In addition, $P_{0\alpha}$ is the partial pressure of component $\alpha$ at concentration $C$ and $\nu^{(3)}_{\alpha\beta}, \nu^{(4)}_{\alpha\beta}$ are the collision frequencies, which can be found in Ref. [18] for the hard sphere molecular system. By using the above procedure, the actual value of the preselected pairs for collision can be deduced.

### 2.3 Sampling of macroscopic quantities

In the DSMC method, the macroscopic quantities in the cells are determined as time averages in the steady state. As a consequence, the number density of the components in the cell is defined by

$$\frac{n_\alpha}{n_0} = \frac{\overline{N}_\alpha V_A}{N_A V_C}, \tag{13}$$

where $N_A$ denotes the total number of particles initially distributed in the upstream reservoir and $V_A$ is the volume of the upstream reservoir. The bar denotes the operation of the time average.

The macroscopic velocity of the components are calculated as

$$\frac{\boldsymbol{u}'_\alpha}{v_0(C_A)} = \frac{1}{N_{T\alpha}}\sum_{i=1}^{N_{T\alpha}}\boldsymbol{v}_{\alpha i}, \tag{14}$$

where $N_{T\alpha}$ is the total number of particles from component $\alpha$ in the cell during the sampling time and $\boldsymbol{v}_{\alpha i}$ is the dimensionless velocity of the i-th molecule from component $\alpha$ in the cell.

Finally, the temperature of the gas is obtained such that

$$\frac{T}{T_0} = \frac{2}{3}\frac{1}{N_T}\sum_{\alpha=1}^{2}\sum_{i=1}^{N_{T\alpha}}\frac{m_\alpha}{m(C_A)}(\boldsymbol{v}_{\alpha i} - \boldsymbol{u})^2 \tag{15}$$

where $N_T = N_{T1} + N_{T2}$ is the total number of particles in the cell during the sampling period. In addition, the dimensionless macroscopic velocity of the mixture is given by $\boldsymbol{u} = (n_1 m_1 \boldsymbol{u}_1 + n_2 m_2 \boldsymbol{u}_2)/(n_1 m_1 + n_2 m_2)$ with $\boldsymbol{u}_\alpha = \boldsymbol{u}'_\alpha / v_0(C_A)$.

### 2.4 Simulation parameters

The parameters in the method are given as follows. The size of the reservoirs is $R_A = R_B = L_A = L_B = 8R$. These reservoir sizes are chosen on the basis of previous experiences and are proved to be optimal for the present simulation. The total number of particles is $2 \times 10^7$, which slightly varies during the simulation. The time step is $\Delta t = 0.005R/v_0(C_A)$. The particular simulations run until a criterion formulated in terms of the statistical scattering of the flow rate is fulfilled. The statistical scattering is given by $\varepsilon = \sqrt{N^+}/(N^+ - N^-)$. Here, $N^+$ and $N^-$ denote the total numbers of particles crossing through the inlet cross section from the upstream reservoir to the tube and in the reverse direction, respectively. The criterion for the simulation is fulfilled with the inequality $\varepsilon < 0.004$. This criterion provides numerical results in terms of the total flow rate with accuracy better than $\pm 0.5\%$.

## 3 Results

In this section, results for the flow rates and the axial distributions of the macroscopic quantities, the rarefaction parameter and the Mach number are presented for the two mixtures under consideration in a wide range of the reference rarefaction parameter and for various pressure and length to radius ratios. The mass and diameter ratios of the mixtures of $He/Xe$ and $Ne/Ar$ are given by $m_1/m_2 = [4.0026/131.30, 20.183/39.948]$ and $d_1/d_2 = [1/2.226, 1/1.406]$.

**TABLE 1**. NORMALIZED FLOW RATES FOR $He/Xe$ IN TERMS OF $\delta_A$ FOR $C_A = 0.5$, $P_B/P_A = 0.1$ and $L/R = [1,5,10]$ (FROM TOP TO BOTTOM).

| $\delta_A$ | $J_1$ | $J_2$ | $J_1/J_2$ | $J$ | $J^*$ |
|---|---|---|---|---|---|
| 0 | 0.351 | 0.0613 | 5.73 | 0.412 | 0.171 |
| 0.1 | 0.348 | 0.0631 | 5.51 | 0.411 | 0.173 |
| 0.5 | 0.335 | 0.0709 | 4.72 | 0.406 | 0.183 |
| 1 | 0.320 | 0.0801 | 3.99 | 0.400 | 0.194 |
| 5 | 0.243 | 0.129 | 1.88 | 0.373 | 0.258 |
| 10 | 0.212 | 0.154 | 1.38 | 0.366 | 0.296 |
| 50 | 0.188 | 0.185 | 1.02 | 0.374 | 0.361 |
| 100 | 0.193 | 0.191 | 1.01 | 0.384 | 0.381 |
| 0 | 0.162 | 0.0272 | 5.95 | 0.189 | 0.0787 |
| 0.1 | 0.160 | 0.0280 | 5.69 | 0.188 | 0.0793 |
| 0.5 | 0.150 | 0.0313 | 4.81 | 0.182 | 0.0821 |
| 1 | 0.141 | 0.0352 | 4.01 | 0.176 | 0.0858 |
| 5 | 0.105 | 0.0604 | 1.74 | 0.165 | 0.116 |
| 10 | 0.101 | 0.0799 | 1.26 | 0.181 | 0.149 |
| 50 | 0.131 | 0.129 | 1.02 | 0.261 | 0.258 |
| 100 | 0.147 | 0.147 | 1.00 | 0.294 | 0.302 |
| 0 | 0.0996 | 0.0174 | 5.72 | 0.117 | 0.0480 |
| 0.1 | 0.0973 | 0.0175 | 5.55 | 0.115 | |
| 0.5 | 0.0914 | 0.0200 | 4.57 | 0.111 | 0.0482 |
| 1 | 0.0843 | 0.0219 | 3.84 | 0.106 | |
| 5 | 0.0615 | 0.0370 | 1.66 | 0.0985 | |
| 10 | 0.0612 | 0.0496 | 1.23 | 0.111 | 0.0906 |
| 50 | 0.0999 | 0.0982 | 1.02 | 0.198 | |
| 100 | 0.120 | 0.120 | 1.00 | 0.240 | |

### 3.1 Flow rates

Tables 1-3 show the flow rates $J_1$ and $J_2$ of each species, the ratio $J_1/J_2$ and the total flow rate $J$ for different flow configurations. The ratio $J_1/J_2$ is used to analyze the separation effect which appears because the components of the mixture due to their different molecular velocities have different average flow speeds in the tube. Also, in some cases the flow rates for single gas flow are provided for comparison purposes.

In Table 1, all these quantities are tabulated for the mixture of $He/Xe$ flowing through channels with $L/R = [1,5,10]$ at $P_B/P_A = 0.1$ in terms of the reference rarefaction parameter, which varies as $0 \leq \delta_A \leq 100$. The concentration is fixed at $C_A = 0.5$. In addition, the total flow rate for a single component gas $J^*$ from Ref. [11] is shown. The single gas result denoted by $W$ in Ref. [11] is converted to our formalism according to $J = W/(2\sqrt{\pi})$. In the top part of Table 1, the results for $L/R = 1$ are shown. The dependency of the flow rates on $\delta_A$ can be observed. It is seen that as $\delta_A$ is increased the flow rates $J_1$, which correspond to $He$, are decreased up to $\delta_A = 50$ and then they are increased, while the flow rates $J_2$, which correspond to $Xe$ are steadily increased. Also, the ratio $J_1/J_2$ is monotonically decreased as $\delta_A$ is increased. This is due to the separation effect and therefore in the hydrodynamic (or viscous) limit, where separation is diminishing, the ratio $J_1/J_2$ tends to the limiting value of $C_A/(1-C_A) = 1$. The fact that the lighter species is traveling faster than the heavier one, becomes more important with increasing gas rarefaction (i.e. with decreasing $\delta_A$), where the gas components become more independent of each other due to the reduction of intermolecular collisions. The total flow rates, compared to the corresponding ones of the single gas, are quite different, except in the case of large values of $\delta_A$, where the total flow rates are approaching to each other. This is because as we are approaching the hydrodynamic limit the gas becomes so dense that diffusion effects become negligible. Furthermore, it is noticed that the dependency of the total flow rate $J$ on $\delta_A$ is not monotonic. As $\delta_A$ is increased, the flow rate is initially reduced and then after some critical value of $\delta_A$ the flow rate is increased. It seems that a type of a Knudsen minimum shows up, although such a minimum is not present in the corresponding single gas flow.

The center and bottom parts of Table 1 present the corresponding flow rates of the species and of the mixture in terms of $\delta_A$ for $L/R = 5$ and 10. It can be clearly seen that the flow rates decrease as the channel becomes longer. This behavior is easily explained by the fact that the local pressure gradient becomes smaller with increasing channel length at constant overall pressure drop. Beyond that the qualitative behavior of the flow rates

**TABLE 2**. NORMALIZED FLOW RATES FOR $He/Xe$ IN TERMS OF $\delta_A$ FOR $C_A = 0.5$, $P_B/P_A = 0.4$ AND $L/R = 1$.

| $\delta_A$ | $J_1$ | $J_2$ | $J_1/J_2$ | $J$ |
|---|---|---|---|---|
| 0 | 0.234 | 0.0406 | 5.78 | 0.275 |
| 0.1 | 0.231 | 0.0425 | 5.43 | 0.273 |
| 0.5 | 0.221 | 0.0491 | 4.51 | 0.271 |
| 1 | 0.211 | 0.0569 | 3.71 | 0.268 |
| 5 | 0.180 | 0.104 | 1.73 | 0.284 |
| 10 | 0.176 | 0.133 | 1.32 | 0.308 |
| 50 | 0.177 | 0.175 | 1.01 | 0.353 |
| 100 | 0.185 | 0.185 | 1.00 | 0.370 |

**TABLE 3**. NORMALIZED FLOW RATES FOR $He/Xe$ (TOP) AND $Ne/Ar$ (BOTTOM) IN TERMS OF $\delta_A$ FOR $C_A = 0.5$, $P_B/P_A = [0.1, 0.4, 0.7]$ AND $L/R = 0.3$.

| | $P_B/P_A = 0.1$ | | | | $P_B/P_A = 0.4$ | | | | $P_B/P_A = 0.7$ | | | |
|---|---|---|---|---|---|---|---|---|---|---|---|---|
| $\delta_A$ | $J_1$ | $J_2$ | $J_1/J_2$ | $J$ | $J_1$ | $J_2$ | $J_1/J_2$ | $J$ | $J_1$ | $J_2$ | $J_1/J_2$ | $J$ |
| 0 | 0.454 | 0.0796 | 5.70 | 0.533 | 0.302 | 0.0525 | 5.76 | 0.355 | 0.151 | 0.0264 | 5.72 | 0.178 |
| 0.1 | 0.451 | 0.0821 | 5.50 | 0.533 | 0.299 | 0.0550 | 5.44 | 0.354 | 0.149 | 0.0279 | 5.35 | 0.177 |
| 0.5 | 0.436 | 0.0917 | 4.76 | 0.528 | 0.289 | 0.0638 | 4.54 | 0.353 | 0.143 | 0.0330 | 4.34 | 0.176 |
| 1 | 0.418 | 0.104 | 4.04 | 0.522 | 0.277 | 0.0742 | 3.73 | 0.351 | 0.137 | 0.0396 | 3.47 | 0.177 |
| 5 | 0.317 | 0.164 | 1.94 | 0.481 | 0.237 | 0.134 | 1.77 | 0.370 | 0.131 | 0.0830 | 1.57 | 0.214 |
| 10 | 0.265 | 0.190 | 1.40 | 0.455 | 0.221 | 0.164 | 1.35 | 0.384 | 0.144 | 0.115 | 1.25 | 0.259 |
| 50 | 0.215 | 0.210 | 1.02 | 0.426 | 0.201 | 0.195 | 1.03 | 0.397 | 0.160 | 0.155 | 1.03 | 0.315 |
| 100 | 0.212 | 0.211 | 1.01 | 0.424 | 0.201 | 0.200 | 1.00 | 0.401 | 0.162 | 0.162 | 1.00 | 0.325 |
| 0 | 0.135 | 0.0961 | 1.40 | 0.231 | 0.0894 | 0.0637 | 1.40 | 0.153 | 0.0447 | 0.0319 | 1.40 | 0.0766 |
| 0.1 | 0.136 | 0.0981 | 1.38 | 0.234 | 0.0908 | 0.0656 | 1.38 | 0.156 | 0.0456 | 0.0331 | 1.38 | 0.0787 |
| 0.5 | 0.140 | 0.107 | 1.31 | 0.246 | 0.0945 | 0.0733 | 1.29 | 0.168 | 0.0481 | 0.0379 | 1.27 | 0.0859 |
| 1 | 0.145 | 0.117 | 1.24 | 0.261 | 0.100 | 0.0825 | 1.21 | 0.183 | 0.0515 | 0.0434 | 1.19 | 0.0949 |
| 5 | 0.170 | 0.163 | 1.05 | 0.333 | 0.141 | 0.136 | 1.04 | 0.276 | 0.0859 | 0.0832 | 1.03 | 0.169 |
| 10 | 0.183 | 0.182 | 1.00 | 0.364 | 0.165 | 0.163 | 1.01 | 0.328 | 0.117 | 0.116 | 1.01 | 0.233 |
| 50 | 0.202 | 0.203 | 1.00 | 0.404 | 0.194 | 0.194 | 1.00 | 0.388 | 0.156 | 0.156 | 1.01 | 0.312 |
| 100 | 0.206 | 0.207 | 0.994 | 0.413 | 0.200 | 0.200 | 1.00 | 0.400 | 0.162 | 0.163 | 1.00 | 0.325 |

of the species and of the mixture with respect to $\delta_A$ is similar as before. However, it is noticed that the rarefaction parameter where the flow rate $J_1$ takes its minimum depends on $L/R$. Regarding the dependency of separation on $L/R$ it is seen that for the same values of $\delta_A$, as we are moving from $L/R = 1$ to $L/R = 5$ the ratio $J_1/J_2$ is increased and then for $L/R = 10$ is decreased.

It is interesting to examine if this specific behavior of the flows rates on gas rarefaction is still observed at smaller pressure drops. Therefore, in Table 2, the normalized flow rates and the ratio $J_1/J_2$ are tabulated in terms of $\delta_A$ for the binary mixture of $He/Xe$ with $C_A = 0.5$, $P_B/P_A = 0.4$ and $L/R = 1$. By comparing the corresponding results of Table 1, it is clearly seen that by reducing the pressure drop the magnitudes of all flow rates are reduced. However, again as we are moving from the continuum to the free molecular regime, the ratios $J_1/J_2$ are increased. Also, $J_1$ and $J_2$, which are very close at $\delta_A = 100$, since $C_A = 0.5$, start to depart from each other as $\delta_A$ is decreased, with the largest deviation occurring at $\delta_A = 0$. With regard to the total flow rate, first $J$ is reduced up to $\delta_A = 1$, where the minimum flow rate is obtained and then it is increased up to $\delta_A = 100$.

In Tables 3, the flow rates and the ratio $J_1/J_2$ of the two different gas mixtures of $He/Xe$ and $Ne/Ar$ are shown for $C_A = 0.5$, $L/R = 0.3$ and $P_B/P_A = [0.1, 0.4, 0.7]$. Starting the comparison with the corresponding flow rates of the light species, it is seen that as $\delta_A$ is increased the flow rate of $He$ is decreased in all cases except for $P_A/P_B = 0.7$ and $\delta_A \geq 10$, while the flow rate of $Ne$ is always increased. The corresponding flow rates of the heavy species, i.e. $Xe$ and $Ar$, are steadily increased in all cases with increasing $\delta_A$. It is seen that with regard to the light species of the two mixtures there are not only quantitative but also qualitative differences. The ratios $J_1/J_2$ in both mixtures are monotonically decreased as the reference rarefaction parameter is increased and finally they are approaching one as the viscous limit is reached. Thus, the separation effect is present in both mixtures. However, since the values of $J_1/J_2$ of $He/Xe$ are much higher than the corresponding ones for $Ne/Ar$ (except for large values of $\delta_A$ where both ratios are close to one), this is a clear indication that separation is stronger for the mixture with the larger molecular mass ratio. Regarding the total flow rates it is seen that in the case of $Ne/Ar$, $J$ is monotonically increased as $\delta_A$ is increased having a qualitative behavior similar to the one of a single gas, while in the case of $He/Xe$ the dependency on the rarefaction parameter is quite different close to the one previously observed of the other $L/R$. It may be interesting to note that in the present case of the

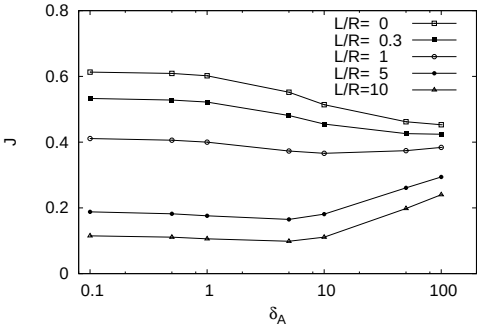


**FIGURE 2**. NORMALIZED TOTAL FLOW RATE FOR $He/Xe$ AS A FUNCTION OF $\delta_A$ FOR $C_A = 0.5$, $P_B/P_A = 0.1$ AND VARIOUS VALUES OF $L/R$.

$He/Xe$ flow through this very short tube, the Knudsen minimum previously observed, does not show up at all for $P_B/P_A = 0.1$ and it very shallow for $P_B/P_A = 0.4$ and 0.7. It is noted that for the $Ne/Ar$ mixture at $P_B/P_A = 0.1$ and $\delta_A = 100$ the computed value of $J_1/J_2$, instead of 1.00, is 0.994. This estimated value is within the expected accuracy of $\pm 0.005$ based on the implemented simulation parameters introduced in Section 2.4 and may be improved if the number of model particles is larger or the termination criterion is more strict, increasing of course in parallel the computational effort.

Closing this subsection on the flow rates, it may be useful to have a visual description of the dependency of the total flow rate of the gas mixture of $He/Xe$ in terms of gas rarefaction and tube length. Therefore, in Fig. 2, the total flow rate $J$ of $He/Xe$ as a function of $\delta_A$ is presented for $C_A = 0.5$, $P_B/P_A = 0.1$ and $L/R = [0, 0.3, 1, 5, 10]$. As $L/R$ is increased the flow rate is decreased. However, it is seen that for very short channels with $L/R \leq 0.3$, the flow rate monotonically decreases with increasing $\delta_A$, while for longer channels, with $L/R \geq 1$, the dependency of the flow rate is not monotonic and the so called Knudsen minimum appears.

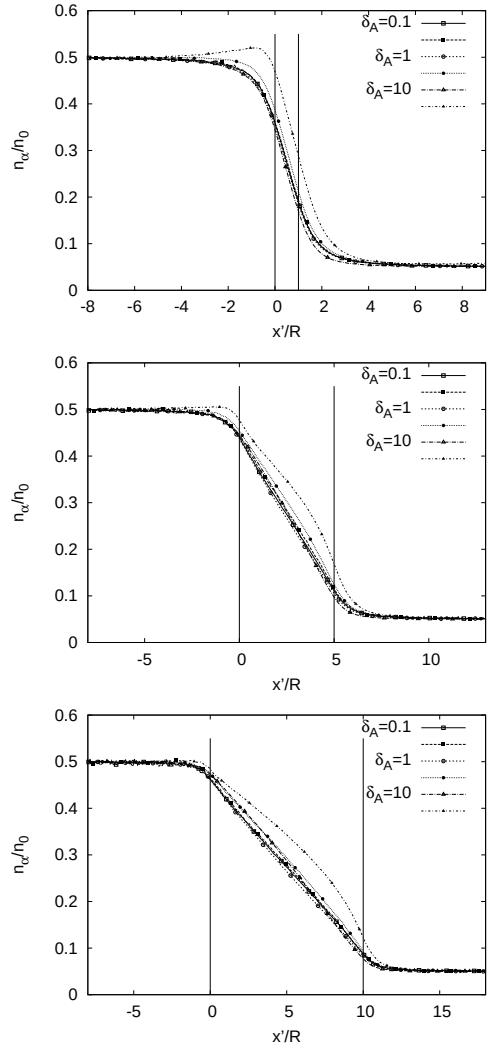


**FIGURE 3**. AXIAL DISTRIBUTIONS OF THE DENSITIES OF EACH SPECIES OF $He/Xe$ FOR $C_A = 0.5$, $P_B/P_A = 0.1$, $\delta_A = [0.1, 1, 10]$ AND $L/R = [1, 5, 10]$ (FROM TOP TO BOTTOM). FILLED AND EMPTY SYMBOLS STAND FOR $He$ AND $Xe$, RESPECTIVELY.

### 3.2 Distributions of macroscopic quantities

Axial distributions of the density of the components of the mixture are presented in Fig. 3. The densities of the components are shown for $He/Xe$ with $C_A = 0.5$, $P_B/P_A = 0.1$, $\delta_A = [0.1, 1, 10]$ and $L/R = 1, 5, 10]$. It can be seen that the component densities vary between the upstream and downstream reference values, exhibiting a strong variation in the tube zone. In the free-molecular limit, the corresponding density profiles of the two species are nearly the same, however at larger values of the rarefaction parameter the densities are component dependent. Because of the difference in the density of the components there is a concentration variation along the flow, while the reference values of $C_A = C_B = 0.5$ far from the tube zone are maintained. This concentration variation is caused by the separation effect. The lighter particle has larger molecular speed than that of the heavier one. When the gas is accelerated, the lighter particles have larger macroscopic velocity, which results into the separation of the components. The separation starting from the inlet of the channel is intensified in the zone of the tube, then the densities tend to the equilibrium values in the outlet reservoirs. As it is seen the effect of the separation phenomena on the number density distributions of each species is more profound in the intermediate rarefaction $\delta_A = 10$ than in the more rarefied atmospheres

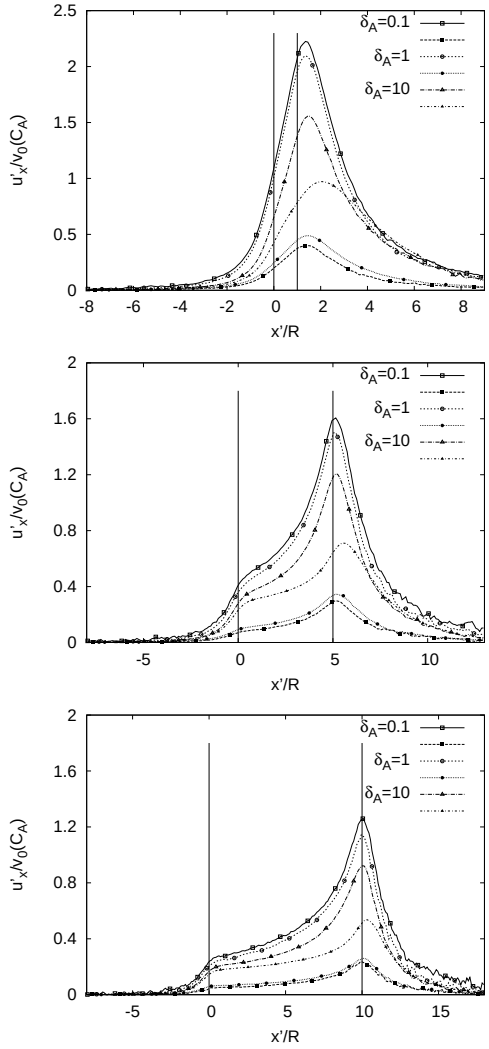


**FIGURE 4**. AXIAL DISTRIBUTIONS OF THE AXIAL VELOCITIES OF EACH SPECIES OF $He/Xe$ FOR $C_A = 0.5$, $P_B/P_A = 0.1$, $\delta_A = [0.1, 1, 10]$ AND $L/R = [1, 5, 10]$ (FROM TOP TO BOTTOM). FILLED AND EMPTY SYMBOLS STAND FOR $He$ AND $Xe$, RESPECTIVELY.

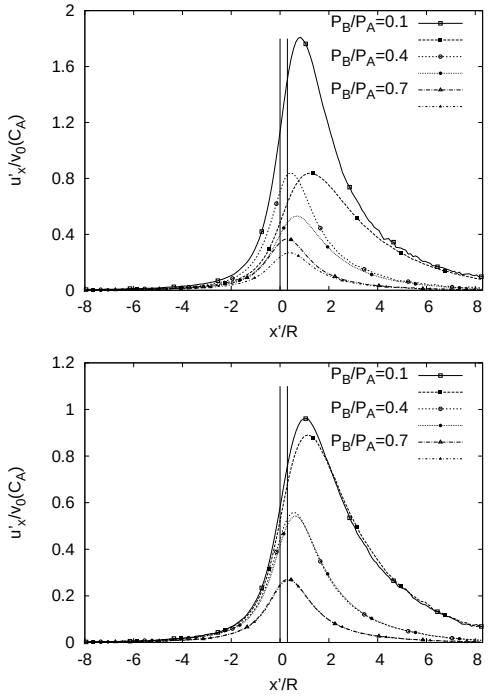


**FIGURE 5**. AXIAL DISTRIBUTIONS OF AXIAL VELOCITIES OF EACH SPECIES OF $He/Xe$ (TOP) AND $Ne/Ar$ (BOTTOM) FOR $C_A = 0.5$, $P_B/P_A = [0.1, 0.4, 0.7]$, $L/R = 0.3$ AND $\delta_A = 5$. FILLED AND EMPTY SYMBOLS STAND FOR $He$ AND $Xe$, RESPECTIVELY.

$\delta_A = 1$ and 0.1. This is an interesting observation which is related to the intermolecular dynamics between the components of the mixture and it is described in [21].

Figures 4 and 5 present the velocity distributions along the axis of the channel. In Fig. 4, the axial velocity distributions of each species are plotted for $He/Xe$ with $C_A = 0.5$, $P_B/P_A = 0.1$, $\delta_A = [0.1, 1, 10]$ and $L/R = [1, 5, 10]$. In all cases the velocities of $He$ are larger than the velocities of $Xe$. The velocity difference between the components becomes larger as the rarefaction parameter decreases. This is due to the fact that the components tend to propagate with their own molecular speeds as the gas becomes more rarefied and intermolecular collisions are less important. In the inlet region and along the channel, the velocities steadily increase reaching their maximum values near the exit of the tube and then they gradually decrease in the outlet section. It is also seen that the velocities become smaller as the channel becomes longer. This is a consequence of the smaller average pressure gradient available with longer channel. It is seen that, in some cases, there is a small fluctuation of the velocity distribution in the downstream reservoir, which is due to the statistical nature of the DSMC since there are fewer particles in the downstream reservoir because of the pressure drop. The fluctuations may be further reduced by increasing the number of model particles or the number of samples. Figure 5 shows the axial velocity profiles of the species of the two mixtures under investigation with $C_A = 0.5$, $P_B/P_A = [0.1, 0.4, 0.7]$, $\delta_A = 5$ and $L/R = 0.3$. The velocity difference between the components of $Ne/Ar$ is smaller than the one of $He/Xe$. It can also be observed that the velocity magnitude is increased with increasing pressure drops.

The temperature distribution for $He/Xe$ with $C_A = 0.5$, $P_B/P_A = 0.1$, $\delta_A = [0.1, 1, 10]$ and $L/R = [1, 5, 10]$ is shown in Fig. 6. It is recalled that the tube wall and the adjacent walls of the two reservoirs are considered as isothermal at constant tem-

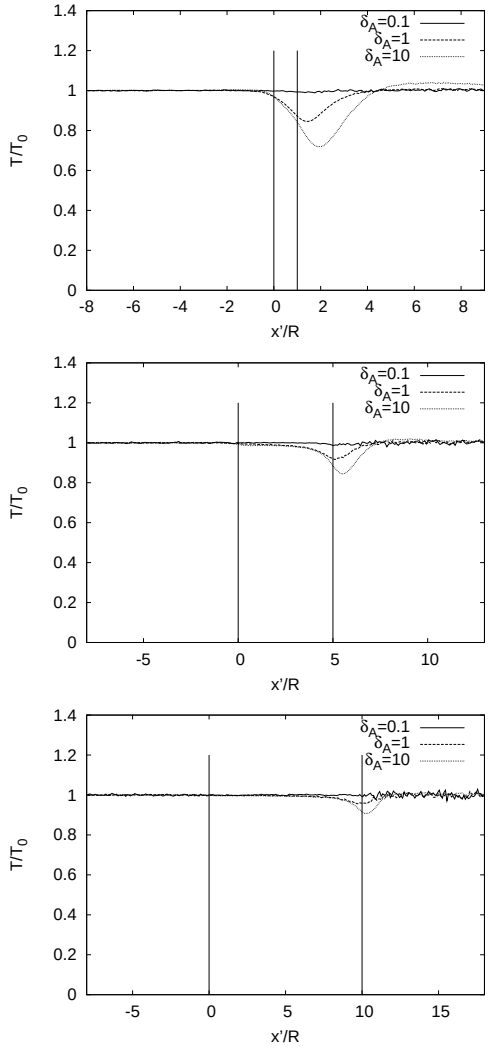


**FIGURE 6**. AXIAL DISTRIBUTIONS OF THE TEMPERATURE OF $He/Xe$ FOR $C_A = 0.5$, $P_B/P_A = 0.1$, $\delta_A = [0.1, 1, 10]$ AND $L/R = 1, 5, 10$ (FROM TOP TO BOTTOM).

perature $T_0$, where the particles-wall interaction is purely diffusive. A temperature drop having its maximum after the exit of the channel is observed. This is due to the strong expansion of the gaseous mixture in the low pressure environment. The temperature drop generally decreases as the channel becomes longer. For longer channels, the flow rates are reduced so the expansion becomes weaker, which eventually causes smaller temperature drop. The small temperature rise seen at $\delta_A = 10$ and $L/R = 1$ in the outlet container has been also observed in corresponding single gas flows [11].

Finally, Fig. 7 shows the axial distribution of the local rarefaction parameter and the Mach number for $He/Xe$ with $C_A = 0.5$, $\delta_A = 1$, $L/R = 5$ and various values of the pressure

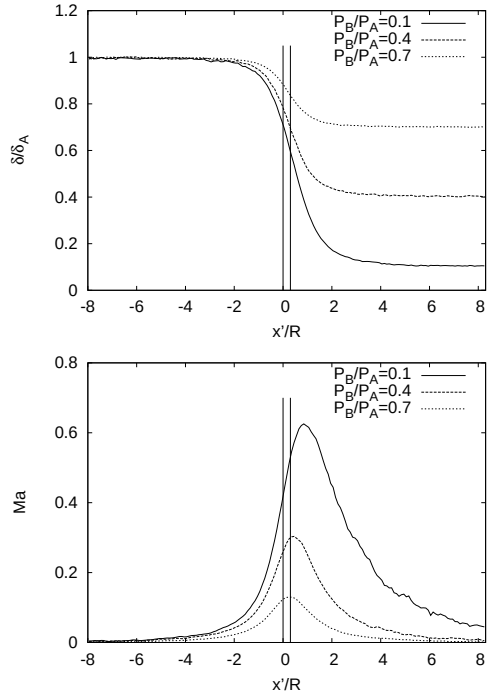


**FIGURE 7**. AXIAL DISTRIBUTIONS OF THE NORMALIZED LOCAL RAREFACTION PARAMETER (TOP) AND THE MACH NUMBER (BOTTOM) OF $He/Xe$ FOR $C_A = 0.5$, $\delta_A = 1$, $P_B/P_A = [0.1, 0.4, 0.7]$ and $L/R = 0.3$.

ratio. The Mach number is defined as $Ma = \sqrt{6/5}u'/v_0(C_A)$, where $u'$ is the absolute value of the mass-density average velocity. It can be seen that the rarefaction parameter shows strong variation along the tube. It starts at the inlet reference value, then decreases in the tube, and finally reaches the outlet value, which is $(P_B/P_A)\delta_A$ in accordance with the pressure drop. This variation is very similar to the variation of number density. With regard to the Mach number, it can be seen that it increases along the flow in the tube, reaching its maximum value just after the exit of the tube, and then starts to decrease. As the pressure drop becomes larger, the Mach number increases, which is in accordance with the observations in Fig. 5.

## 4 Concluding remarks

Rarefied binary gas flows through short tubes have been studied by using the DSMC method. The investigation refers to two types of mixtures having different molecular mass ratios, namely $He/Xe$ and $Ne/Ar$. The flow configuration covers channel lengths from $L/R = 0.3$ to 10, a wide range of the rarefaction parameter from the free molecular limit up to the slip regime and various values of the pressure drop. The flow rates of each species and of the mixture as well as the axial distributions of

density, axial velocity and temperature together with the rarefaction parameter and the Mach number have been presented. The dependency of the results on the geometry, flow and mixture parameters is examined in detail. The differences of the flow behavior compared to the single gas case is more pronounced for the $He/Xe$ mixture, which has a molecular mass ratio much larger than the one of $Ne/Ar$. It is found that as the gas rarefaction parameter is increased the $He/Xe$ flow rate for very short channels may be monotonically decreased and for longer channels it may exhibit the Knudsen minimum phenomenon, while the corresponding $Ne/Ar$ and single gas flow rates are steadily increased. This behavior also depends on the pressure ratio. Overall, the present work provides a systematic investigation of rarefied binary flows through short tubes, and the results can be valuable in the design of gaseous microfluidic and vacuum devices.

## ACKNOWLEDGMENT

The present research obtained financial support from the European Community's Seventh Framework programme (FP7/2007-2013) under grant agreement no 215504.

## REFERENCES

[1] Hanks, R.W., and Weissberg, H.L., 1964. Slow viscous flow of rarefied gases through short tubes. J. Appl. Phys. **35**, pp. 142-144.

[2] Sreekanth, A.K., 1965. Transition flow through short circular tubes. Phys. Fluids **8**, pp. 1951-1956.

[3] Borisov, S. F., Neudachin, I. G., Porodnov, B. T., and Suetin, P. E., 1973. Flow of rarefied gases through an orifice for small pressure drop. Zh. Tekh. Fiz. **43**, pp. 17351739.

[4] Porodnov, B. T., Suetin, P. E., Borisov, S. F., and Akinshin, V. D., 1974. Experimental investigation of rarefied gas flow in different channels. J. Fluid Mech. **64**, pp. 417-437.

[5] Fujimoto, T., and Usami, M., 1984. Rarefied gas flow through a circular orifice and short tubes. Trans. ASME: J. Fluids Eng. **106**, pp. 367373.

[6] Usami, M., and Okuyama, K., 1999. Molecular simulation of rarefied supersonic free jets by DSMC method. JSME Int. J. B-Fluids and Thermal Eng. **42**, pp. 369-376.

[7] Shinagawa, H., Setyawan, H., Asai, T., Yuuichi, Y., and Okuyama, K., 2002. An experimental and theoretical investigation of rarefied gas flow through circular tube of finite length. Chem. Eng. Sci. **57**, pp. 4027-4036.

[8] Lilly, T.C., Gimelshein, S.F., Ketsdever, A.D., and Markelov, G.N., 2006. Measurements and computations of mass flow and momentum flux through short tubes in rarefied gases. Phys. Fluids **18**, pp. 093601-11.

[9] Sharipov, F., 2004. Numerical simulation of rarefied gas flow through a thin orifice. J. Fluid Mech. **518**, pp. 35-60.

[10] Varoutis, S., Valougeorgis, D., Sazhin, O., and Sharipov, F., 2008. Rarefied gas flow through short tubes into vacuum. J. Vac. Sci. Technol. A **26**, pp. 228-238.

[11] Varoutis, S., Valougeorgis, D., and Sharipov, F., 2009. Gas flow through tubes of finite length over the whole range of the rarefaction for various pressure drop ratios. J. Vac. Sci. Technol. A **27**, pp. 1377-1391.

[12] Sharipov, F., 1999. Rarefied gas flow through a long rectangular channel. J. Vac. Sci. Technol. A **17**, pp. 3062-3066.

[13] Graur, I., and Sharipov, F., 2007. Gas flow through an elliptical tube over the whole range of the gas rarefaction. Eur. J. Mech. B/Fluids **27**, pp. 335-345.

[14] Graur, I., and Sharipov, F., 2008. Non-isothermal flow of rarefied gas through a long pipe with elliptic cross section. Microfluid. Nanofluid. **6**, pp. 267-275.

[15] Szalmas, L., and Valougeorigs, D., 2010. A fast iterative model for discrete velocity calculations on triangular grids. J. Comp. Phys., **229**, pp. 4315-4326.

[16] McCormack, F.J., 1973. Construction of linearized kinetic models for gaseous mixtures and molecular gases. Phys. Fluids, **16**, pp. 2095-2105.

[17] Kosuge, S., 2009. Model Boltzmann equation for gas mixtures: Construction and numerical comparison. Eur. J. Mech. B/Fluids **28**, pp. 170-184.

[18] Sharipov, F., and Kalempa, D., 2002. Gaseous mixture flow through a long tube at arbitrary Knudsen number. J. Vac. Sci. Technol. A, **20**, pp. 814-822.

[19] Naris, S., Valougeorgis, D., Kalempa, D., and Sharipov, F., 2004. Discrete velocity modelling of gaseous mixture flows in MEMS. Superlattices Microstruct. **35**, pp. 629-643.

[20] Naris, S., Valougeorgis, D., Kalempa, D., and Sharipov, F., 2005. Flow of gaseous mixtures through rectangular microchannels driven by pressure, temperature and concentration gradients. Phys. Fluids **17**, pp. 100607.1-12.

[21] Szalmas, L., and Valougeorgis, D., 2010. Rarefied gas flow of binary mixtures through long channels with triangular and trapezoidal cross sections. Microfluid. Nanofluid. **9**, pp. 471-487.

[22] Szalmas, L., Pitakarnnop, J., Geoffroy, S., Colin, S., and Valougeorgis, D., 2010. Comparative study between computational and experimental results for binary rarefied gas flows through long microchannels. Microfluid. Nanofluid. **9**, pp. 1103-1114.

[23] Bird, G. A., 1994. Molecular Gas Dynamics and the Direct Simulation of Gas Flows. Oxford University Press, Oxford.

[24] Wagner, W., 1992. A convergence proof for Bird's direct simulation Monte Carlo method for the Boltzmann equation. J. Stat. Phys. **66**, pp. 1011-1044.

[25] Dietrich, S., and Boyd, I.D., 1996. Scalar and parallel optimized implementation of the direct simulation Monte Carlo method. J. Comp. Phys. **126**, pp. 328-342.

[26] Bird, G.A., 2005. The DS2V/3V Program Suite for DSMC Calculations. AIP Conf. Proc. **762**, pp. 541-546.